Environmental Nanotechnology, Monitoring & Management 5 (2016) 44–53

Contents lists available at ScienceDirect

Environmental Nanotechnology, Monitoring & Management

journal homepage: www.elsevier.com/locate/enmm

Photocatalytic degradation of low density polyethylene (LDPE) films using titania nanotubes

Saba Sadaqat Ali[a,*], Ishtiaq A. Qazi[a], Muhammad Arshad[a], Zahiruddin Khan[a], Thomas C. Voice[b], Ch. Tahir Mehmood[a]

[a] Institute of Environmental Science and Engineering, School of Civil and Environmental Engineering, National University of Sciences and Technology, Sector H-12, Islamabad 44000, Pakistan
[b] Department of Civil and Environmental Engineering, Michigan State University, East Lansing, MI, USA

ARTICLE INFO

Article history:
Received 13 September 2015
Received in revised form
20 December 2015
Accepted 4 January 2016

Keywords:
Titania
Low density polyethylene
Photocatalytic degradation
Titania nanotubes
Dye sensitization

ABSTRACT

Polyethylene (PE) waste disposal is a major issue now a days that poses serious threats to human and environmental health. Among the methods of dealing with problem, photocatalytic degradation in the visible light is an alternative option that has received attention recently. The photo catalyst, generally used, is titania in the nanoparticle form. In the current study, complexity of employing a larger surface area nanomaterial in the form of titania nanotubes has been investigated. Prepared nanostructures were characterized by SEM, EDS, XRD, BET surface area measurements and UV-visible spectroscopy. Taking a lead from the work done for the development of dye sensitized solar cells, blue green dye was used to sensitize the TNTs with very encouraging results. The degradation of pure and composite PE films was measured in terms of photo-induced weight loss and was confirmed by FTIR, SEM, surface roughness and tensile strength testing. Thus, polyethylene films with 10% dye sensitized titania nanotubes showed a degradation of around 50% under visible light over a short period of 45 days.

1. Introduction

Excessive use of plastics in domestic, industrial and agriculture sectors exert pressure on capacities available for plastic waste disposal which cause an additional burden on the environment (Shah et al., 2008; Zan et al., 2006). Plastics including shopping bags, prepared from polyethylene (PE), after their useful life, find their way to streets, sidewalks, beaches and water bodies ultimately to the block sewerage system which may serve as a suitable habitat for disease causing vectors including mosquitoes (Njeru, 2006) and lead to the death of billions of marine animals by ingestion of the plastic debris or entanglement (Sheavly and Register, 2007).

A number of approaches have been proposed for dealing with the plastic waste. These include incineration, landfills, thermal degradation, bio-degradation and photo-catalysis (Singh and Sharma, 2008). Many of these are associated, however, with secondary problems. Uncontrolled burning of polyethylene produces vapors which includes many toxic compounds like ketones, acrolein, and methane and pollute the air which causes serious environmental hazards (Briassoulis et al., 2004; Briassoulis, 2006). Polyethylene wastes buried in soil cause negative effects to soil quality and may affect the drainage patterns leading to declined agricultural yield (Seymour, 1989).

Thus, attention has been focused on alternative means of degrading the plastic material, in general, and polyethylene in particular. These include thermal, catalytic, mechano-chemical, ozone induced and photo-oxidative degradation. Out of all methods, photocatalytic degradation of polymers such as PE has stands out as the most promising (Kim et al., 2006; Chakrabarti et al., 2008; Zhao et al., 2008; Asghar et al., 2011; Mehmood et al., 2015). Photocatalysis using nanostructures as photocatalysts could thus be encouraging and environmental friendly way to tackle the PE problem (Yuan et al., 2013).

Among various types of photocatalysts, TiO_2 (commonly known as Titania) is extensively used for degradation of organic pollutants (Gelover et al., 2004). Titania is a promising photocatalyst due to its high photoactivity, high stability, low cost and absence of toxicity (Fostier et al., 2008). The use of titania as a photocatalyst has also been reported for polyethylene degradation with considerable success (Zan et al., 2006; Zhao et al., 2008, 2006; Zhiyong et al., 2007; Asghar et al., 2010; Thomas et al., 2013; Liang et al., 2013).

* Corresponding author.
E-mail address: sabasadaqat@iese.nust.edu.pk (S.S. Ali).

http://dx.doi.org/10.1016/j.enmm.2016.01.001

For a catalyst in general and the photocatalyst in particular, the active surface area is of critical importance. In the PE degradation studies reported so far titania has been used in the form of nanoparticles. An option for using a larger surface area material, in the form of nanotubes, however, exists (da Silva et al., 2015).

Titania nanotubes (TNTs) are now gaining importance in the process of photo-catalysis (Latif et al., 2014) due to their exceptional chemical and physical properties like high surface area, photo catalytic activity, widespread accessibility and ease of production by an easy and efficient hydrothermal method under moderate conditions of pressure and temperature (Wong et al., 2011). Another issue of concern is that TiO_2 is active only in the UV wavelength range below 385 nm which is less than 5% of solar light. Significant efforts have been made to utilize visible part of solar light and to alter the photocatalytic properties of TiO_2 also as doping of nanomaterials with metals (Kato et al., 2005).

Dye sensitization significantly enhance the photocatalytic activity of the titania nanostructures which has been applied for the fabrication of solar cells (Wang and Lin, 2009; Macák et al., 2005). Dye sensitization is also an efficient method to enhance the photo response of TiO_2 in the visible range of spectrum and has been effectively used for environmental applications (Chowdhury et al., 2012; Vinu et al., 2010; Chatterjee and Mahata, 2001; Chatterjee et al., 2006). BG dye also called emerald green, or malachite green has been used in industry such as paper production to color paper towels and to dye silk. Brilliant green dye (BG, bis (4-diethylaminophenyl)phenylmethylium chloride) has been used to sensitize titania monoliths (Tomás et al., 2008).

2. Materials and methods

2.1. Reagents

Cyclohexane (Merck, Germany), Hydrochloric Acid, Sodium Hydroxide, General Purpose Reagent (GPR) TiO_2 (Sigma–Aldrich Laborchemikalien) and brilliant green dye (chemical formula = $C_{27}H_{34}N_2O_4S$; Dye content = 90%, Molecular Weight 482.63 g/mol) from Sigma Aldrich were used without further purification. Low-density polyethylene (LDPE) pellets having a melting point 115 °C and density 0.93 g/cm^3 were purchased from the local market.

2.2. Synthesis of TiO_2 nanostructures and PE films

25 g GPR was taken in distilled water and stirred for 24 h on a magnetic plate. The resulting solution was then dried in oven at 105 °C for 12 h. The dried sample was then crushed and calcined in a muffle furnace at 450 °C for 6 h to get TNPs in anatase phase (Khan et al., 2013).

Pure TNTs were synthesized by the hydrothermal method where 2.5 g prepared TNPs were added in 100 ml of 10 M NaOH solution and stirred for 2 h followed by 1 h ultra-sonication. The resulting material was transferred into Teflon lined autoclave under pressure at 135 °C for 24 h with continuous stirring. Sample was extracted, cooled at room temperature and washed with 0.1 N HCl and then distilled water several times until the pH of the solution became neutral (6.5–8). After washing, the solution was dried in hot air oven for 24 h at 105 °C. The sample was then ground into fine powder and calcinated at 500 °C for 6 h in order to obtain highly crystalline TNTs (Asapu et al., 2011; Latif et al., 2014).

The dye sensitized photocatalyst was prepared by adding 500 mg of TNPs or TNTs in a saturated solution of brilliant green dye. Suspension was stirred on magnetic stirrer for 24 hours in dark to homogenize the dye and achieve the absorption equilibrium. TNPs/TNTs were filtered, washed with DW and dried (Chatterjee and Mahata, 2001; Macák et al., 2005).

Table 1
Details of pure and composite LDPE films.

Sr #		% of Nanostructres by weight in PE films	Weight (gm)	Thickness (mm)
1	Pure LDPE	–	0.0150	0.024
2	TNPs	1%	0.0201	0.030
3		2%	0.0172	0.025
4		7%	0.0171	0.029
5		10%	0.0194	0.026
7	TNTs	1%	0.0187	0.020
8		2%	0.0184	0.025
9		7%	0.0221	0.023
10		10%	0.0205	0.025
11	BG-TNPs	1%	0.0197	0.027
12		2%	0.0113	0.023
13		7%	0.0204	0.029
14		10%	0.0204	0.028
16	BG-TNTs	1%	0.0194	0.026
17		2%	0.0197	0.024
18		7%	0.0194	0.022
19		10%	0.0197	0.022

Pure polythene films were prepared by dissolving 0.5 g of LDPE beads in 50 mL cyclohexane at 70 °C under continuous stirring for 90 min. 10 mL of the LDPE suspension was spread on glass petri plate to get pure LDPE film. Composite LDPE films were prepared by dissolving the required amount of TNPs, TNTs or Dye sensitized TNPs in the LDPE suspension and after one hour ultra-sonication, 10 mL of each combination was spread on different glass petri plates. All films were dried for 20 min at 70 °C and kept at room temperature for 48 h (Asghar et al., 2011). Details of pure and composite LDPE films are given in Table 1. Weight of the resulting composite was around 0.02 g and thickness was about 0.024 mm. LDPE films were cut into 3 cm × 3 cm square pieces and exposed to UV or visible light for degradation experiments.

2.3. Experimental setup

Photo-degradation of LDPE and composite films was carried out under UV light for 15 days in ambient air with a distance of 5 cm from the light source. After getting expected results under UV light, visible light experiments were carried for 45 days under the same conditions. Films were constantly irradiated in a closed wooden box containing lamp (90 cm × 50 cm × 50 cm) as displayed in Fig. 1. For photo-catalytic experiments, two 18W ultraviolet lamps (primary wavelength of 315 nm) were also used for photo-catalytic activity in UV range and visible lamps of 85 watt with a wavelength range of 400–700 nm were used as light source. ABM Model 150 digital intensity meter was used for light intensity measurement. Light intensity was 2.54 mW/cm^2 for UV lamps and 6.76 mW/cm^2 for visible lamp measured at 5 cm away from sources. A set of films was also kept under dark. Each sample was weighed at regular time intervals.

2.4. Characterization

Surface morphology and size range of titania nanostructures were characterized by scanning electron microscope (JEOL JSM-6460). Energy dispersive spectroscopy (EDS) analytical technique was used to obtain spectra of TNPs and TNTs by using JEOL JSM 6490A analytical station to analyze the elemental composition. X-Ray Diffraction Analysis was used for phase identification of TNPs and TNTs by using JEOL JDX-II X-ray diffractometer. The scanning was done between 10° to 80° at a rate of 5° per minute using Cu-Kα radiation (λ = 0.15478 nm) at an angle of 2θ. Standard conditions for XRD measurements were; room temperature, radiation at

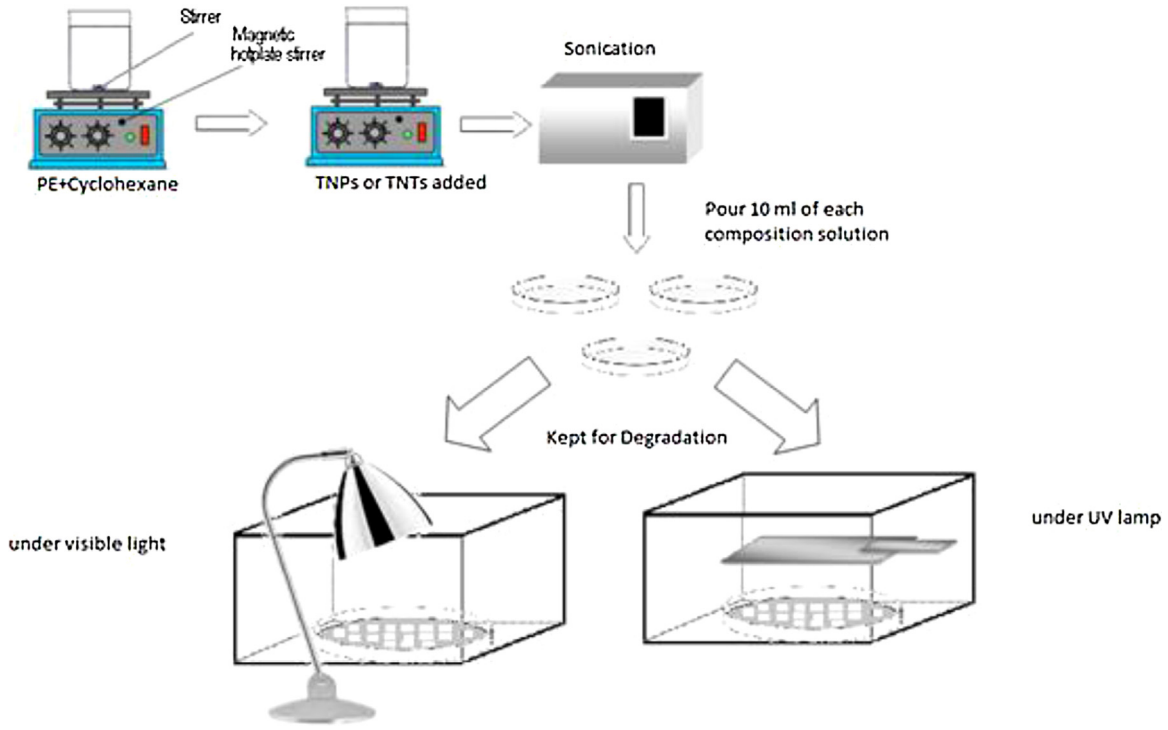

Fig. 1. Experimental setup for photocatalytic degradation of LDPE films.

voltage of 40 keV and 30 mA of current. The X-ray diffraction patterns helped to get crystalline size based on the Scherer equation (Kim et al., 2001).

$$L = \frac{k\lambda}{\beta\cos\theta}$$

UV–vis spectrophotometer ((SQ-2800 Unico) was used for measuring the absorbance of pure and dye sensitized nanoparticles and nanotubes. Micromeritics Gemini VII BET surface area Analyzer was used to measure the pore size and specific surface area of TNPs and TNTs. For BET analysis TNTs or TNPs samples were first degassed at 130 °C for 4 hours under vacuum (Akarsu et al., 2006).

Tensile testing was done to determine the strength of LDPE films before and after irradiation. The testing procedure was followed according to ASTM 882-85. Universal Testing machine (Schimadzu AG XPlus 20kN) was used for this testing. UV–vis spectrophotometer (T 60PG instruments) was used for measuring the absorbance of films before and after irradiation.

Nanovea 2d Optical profilometer PS50 was used to measure the surface roughness of LDPE films before and after irradation. Surface morphologies of pure and composite films before and after irradiation were characterized by scanning electron microscope (JEOL JSM-6460).

To study the weight loss during photocatalytic degradation of LDPE and composite films, weighing balance with 0.0001 gm sensitivity (Schimadzu Model ATY-224) was used for weight measurements. The percentage mass loss was determined by this formula:

$$\%\ \text{Mass loss} = \frac{m_i - m_f}{m_i} \times 100$$

where m_i = Initial weight before irradiation m_f = Final weight after irradiation

FTIR spectra of LDPE and composite films were obtained using Perkin Elmer Spectrum FTIR spectromete to determine molecular changes before and after irradiation. Degradation rates were calculated by using the standard carbonyl index method.

3. Results and discussion

3.1. Characterization of nanostructures and LDPE films

Fig. 2(a and b) shows the XRD results of nanoparticles and nanotubes respectively. These graphs are obtained by powder XRD technique using Cu-Kα radiations at an angle of 2θ from 10° to 80° with a scanning step size of 0.021°. The presence of four main peaks at 2θ values of 25.3°, 36.9, 48.04° and 55.07° indicates that TNPs and TNTs are in anatase phase and highly crystalline in nature. Energy Dispersive Spectroscopy (EDS) Analysis in Fig. 2(c and d) shows that major constituents for pure TNPs and TNTs are Titanium and Oxygen i.e. approximately 43% and 56% in TNPs and 41% and 57% in TNTs respectively. BET analysis of pure TNPs and TNTs revealed, at Standard Temperature and Pressure (STP) shows the surface area of pure TNPs as 81 m^2/g and 161 m^2/g for TNTs.

3.2. Tensile strength testing

Tensile testing was done to determine the strength of films. The testing procedure was followed according to ASTM 882-85 with using Universal testing machine (Schimadzu AG XPlus 20 kN). LDPE films with a gauge length of 30 mm and width of 10 mm were cut from the films and run at a speed of 1 mm/min for tensile strength measurements. The average value is presented for each sample. Addition of nanostructure modifies the mechanical properties of LDPE composites which can be seen from their elongation at break (εb) average values for each sample, as reported in Table 2. Tensile strength is calculated by this formula and final results are expressed in Megapascals (MPa).

$$\text{Tensile Strength} = \frac{\text{load at break}}{\text{original width} \times \text{original thickness}}$$

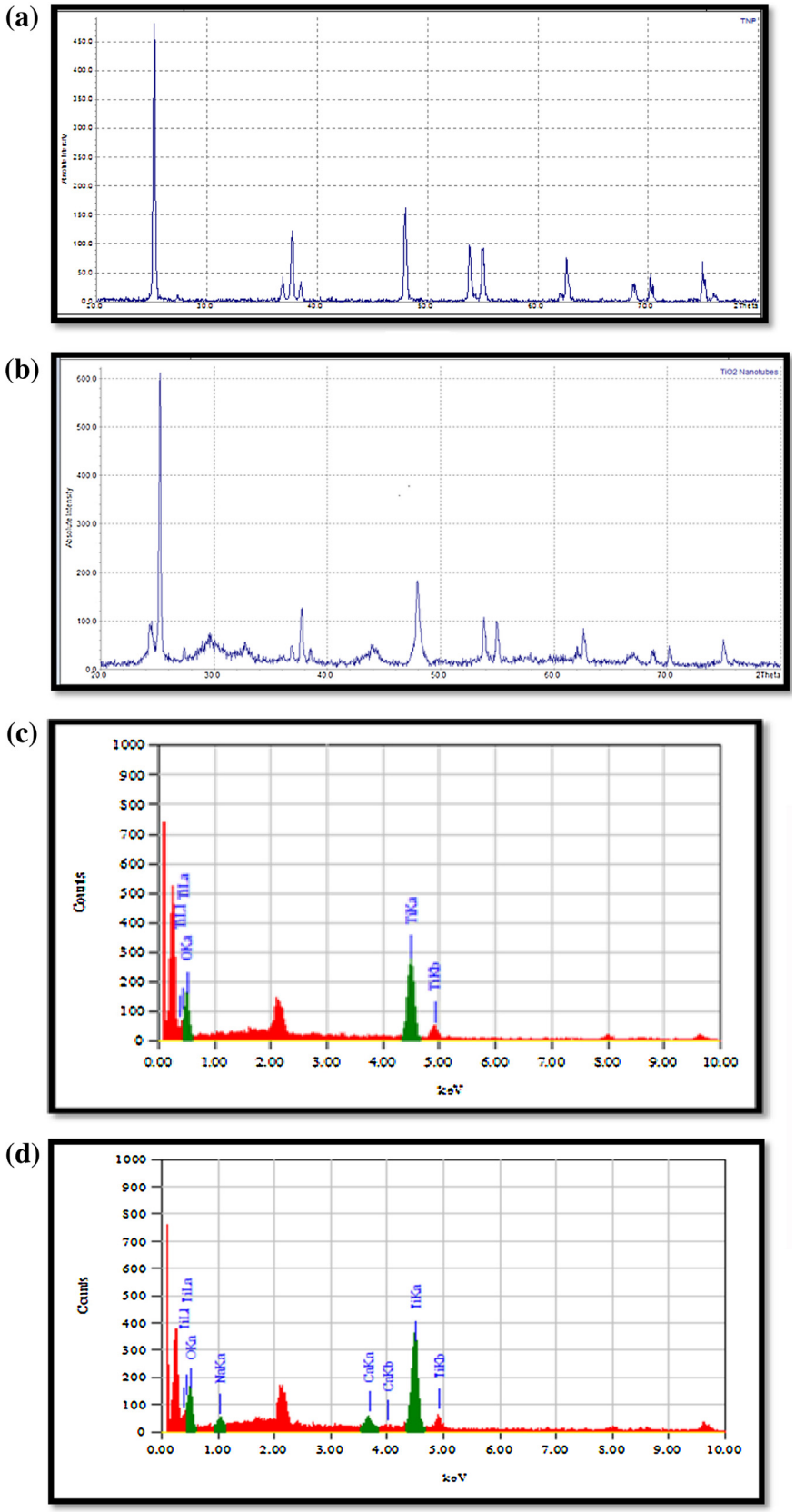

Fig. 2. (a) XRD Intensity plot for pure Titania Nanoparticles (b) XRD Intensity plots of Titania Nanotubes (c) EDS Spectra of nanoparticles (d) EDS Spectra of nanotubes.

Percent elongation is measured by;

$$\%\ \text{Elongation} = \frac{\text{Elongation at rupture} \times 100}{\text{Initial gage length}}$$

It can be interpreted that film degradation has a negative effect on the tensile strength of films. Addition of nanostructures also affect tensile properties of LDPE films as density of PE increases,

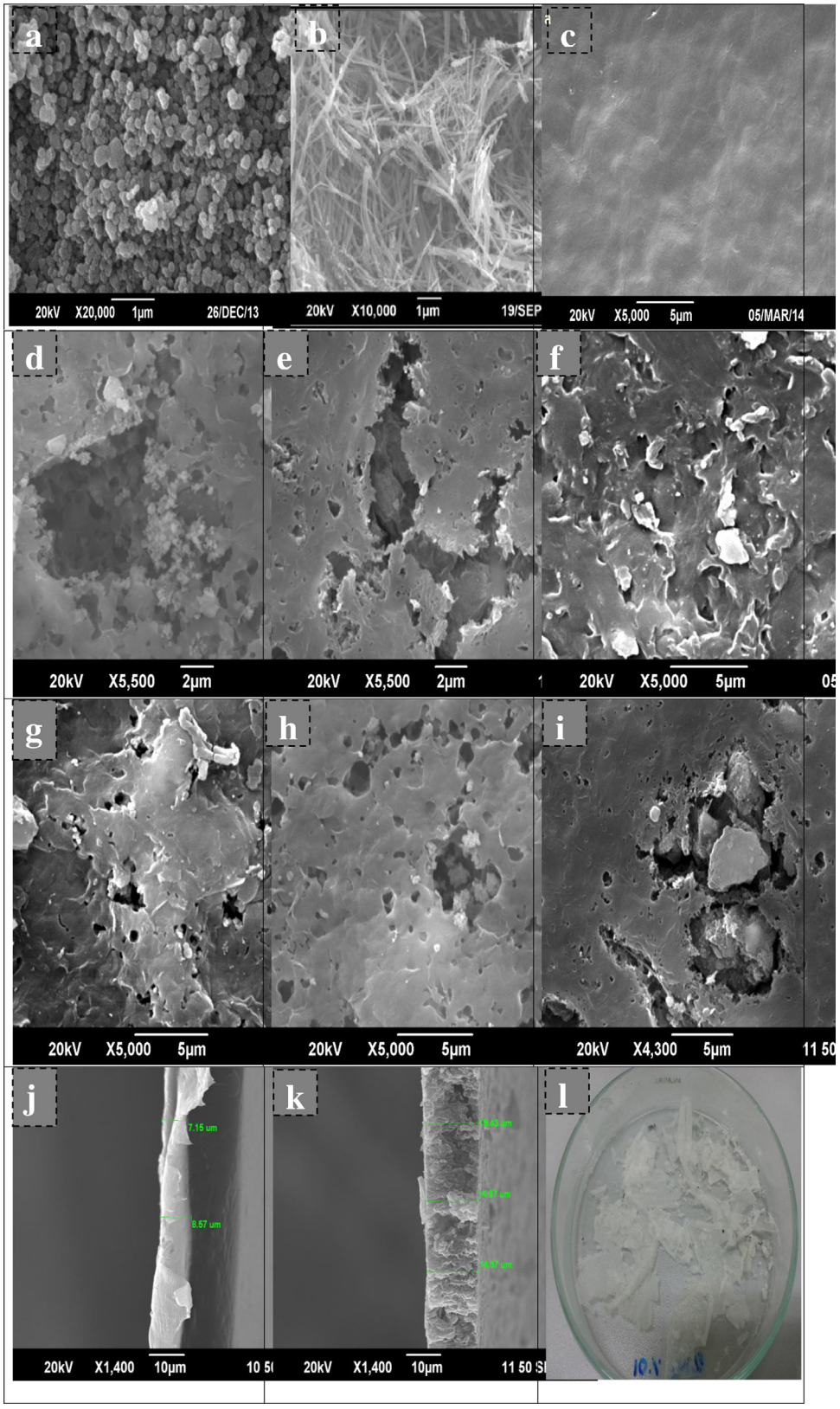

Fig. 3. (a) SEM images of nanoparticles (b) nanotubes (c) Pure LPPE before exposure d) LDPE-TNPs composites after UV exposure e) LDPE-TNTs composites after UV exposure (f) LDPE-TNPs film visible light irradiated for 45 days (g) BG-TNPs film visible light irradiated for 45 days (h) LDPE-TNTs films visible light irradiated for 45 days (i) BG-TNTs film visible light irradiated for 45 days (j) LDPE composite films thickness containing 2% TNTs before visible light irradiation (k) LDPE composite films thickness containing 2% TNTs after visible light irradiation for 45 Days (l) Degraded LDPE films containing TNTs under Visible light.

Table 2
Tensile strength and elongation values for pure and composite LDPE films before and after visible irradiation.

Sample composition	Tensile strength(MPa)		Break elongation (%)	
	Before	After	Before	After
Pure LDPE	10.2	9.8	3.53	3.41
LDPE + 2%TNPs	8.88	3.37	7.31	3.19
LDPE + 7%TNPs	8.37	0.92	3.12	1.95
LDPE + 2%TNTs	14.7	2.17	7.37	1.52
LDPE + 7%TNTs	8.81	1.84	7.12	1.73

Table 3
Weight loss data (under UV for 15 days) after applying exponential equation.

Titania concentration in percentage (w/w)	W_o (gm)	k	R^2	$\lambda_{1/2}$ (days)
0%	0.0176	0.0003	0.9912	2310
1%TNPs	0.0205	0.001	0.9913	693
2%TNPs	0.0191	0.002	0.989	346
7%TNPs	0.0216	0.004	0.8952	173
10%TNPs	0.0198	0.004	0.9194	173
1% TNTs	0.0184	0.001	0.9696	693
2%TNTs	0.0197	0.003	0.914	231
7%TNTs	0.0229	0.005	0.922	138
10%TNTs	0.0196	0.006	0.994	115

Table 4
Weight loss data (under visible light for 45 days) after applying exponential equation.

Titania concentration in percentage (w/w)	W_o (gm)	k	R^2	$\lambda_{1/2}$ (days)
0%	0.0150	0.00009	0.593	7700
1% TNPs	0.0201	0.0009	0.8738	770
2% TNPs	0.0172	0.001	0.8774	693
7% TNPs	0.0171	0.001	0.8895	693
10% TNPs	0.0194	0.002	0.8823	346
1% BGTNPs	0.0197	0.001	0.8728	693
2% BGTNPs	0.0113	0.001	0.8576	693
7% BGTNPs	0.0204	0.002	0.8872	346
10% BGTNPs	0.0204	0.003	0.8818	231
1% TNTs	0.0187	0.001	0.8855	693
2%TNTs	0.0184	0.001	0.8898	693
7%TNTs	0.0221	0.002	0.8833	346
10%TNTs	0.0205	0.003	0.8752	231
1% BGTNTs	0.0194	0.001	0.8663	693
2% BGTNTs	0.0197	0.002	0.8849	346
7% BGTNTs	0.0194	0.002	0.899	346
10% BGTNTs	0.0197	0.004	0.8815	173

tensile strength increases while elongation percent decreases. The high percentage of TNPs or TNTs causes agglomeration in PE and ultimately cause loss of tensile strength as nanostructures agglomeration in PE matrix cause some morphological alterations (Fa et al., 2010). Elongation also correlates with the formation of carbonyl groups as during degradation as carbonyl ratio increases, percent elongation decreases. Films containing 7% titania nanostructures showed maximum elongation loss and tensile strength decline after 45 days of irradiation. The films degraded after UV radiation broke down on touching and were so fragile that tensile testing could not be performed on these films.

3.4. Weight loss measurements

LDPE film weight reduction measurements was carried out to study their photo-degradation. Fig. 5(a and b) displays the photo induced weight loss of different samples with UV and visible light irradiation, respectively. The values of '*k*' for each titania concentration (0–10%), values of the *Correlation Coefficient* 'R^2' and half-life of each composite are tabulated in Tables 3 and 4. Weight loss data was plotted again time (d) and exponential equation was fitted on it as first order kinetics

$$\frac{dW}{dt} = -kt \quad (1)$$

With '*k*' as the '*degradation rate constant*' and, W_o as the weight at day '0' (the start of the disintegration process), integration of the equation leads to Eq. (2).

$$W = W_o e^{kt} \quad (2)$$

After UV irradiation, the noticeable degradation rate shows a maximum at films containing 10% TNTs which is 78% by weight and 67% in case of 10% TNPs in 15 days which showed that nanotubes are effective for photocatalytic degradation of LDPE (Fig. 5a).

Pure LDPE films showed no noticeable weight loss after visible irradiation but TNP embedding in LDPE matrix leads to the weight loss of films. In the case of LDPE composites with pure TNPs (10%) exposed to visible light, (Fig. 5b) the weight of films was reduced to almost 41% after 45 days. On the other hand, after 45 days of exposure to visible light, almost 48% of the LDPE-10% TNTs composites were degraded. Also, the weight loss rate for those films which contain brilliant green (BG) dye sensitized TNPs or TNTs is higher than LDPE films containing pure TNPs or TNTs. Similarly, composite films containing BG sensitized TNTs showed faster degradation rate under visible light as compare to BG-TNPs composites.

Table 5
Surface roughness values for pure and composite LDPE films before and after irradiation.

LDPE films composition	% Surface roughness (R_a)		
	Before	After visible (after 45 days)	After UV (15 days)
LDPE	0.52	0.79	0.91
LDPE + 2% TNPs	0.64	0.88	0.99
LDPE + 10%BG-TNPs	1.04	1.68	–
LDPE + 2%TNTs	0.56	1.22	1.42
LDPE + 10%TNTs	0.93	1.98	2.83
LDPE + 10%BG-TNTs	1.05	1.84	–

3.5. Surface morphology

3.5.1. Surface roughness measurement

Contact profilometry provided 2D measurements of surface roughness at the micrometer order. The test samples were LDPE composite films 3 × 3 cm in area. Contact profilometry of films quantify the morphology of fractures and surface irregularities in their surfaces before and after irradiation. For a given test line, the roughness was measured as the arithmetical mean of peaks above and under the baseline (Chappard et al., 2003). The mean roughness (Ra) was calculated from several samples according to ISO 8247 and their roughness is tabulated in Table 5. Maximum change in roughness was observed in 10% dye sensitized TNTs composite films. Films were smooth and plane before degradation, but photo induced weight loss caused fractures and holes in films due to which the surface roughness increased.

3.5.2. SEM analysis

Fig. 3(a and b) shows the images of TNPs and TNTs taken by Scanning electron microscope. The diameter of spherical particles ranges from 40 to 80 nm with an average value of 50 nm. The average diameter of nanotubes is 40 nm. TNTs are in the form of tubular clusters not completely separated from each other and exhibit high surface area as compare to nanoparticles. These images show that the size of nanoparticles and nanotubes are good enough to use in our experiments. SEM image of pure LDPE films before light exposure is shown in Fig. 3c. SEM images of TNPs and TNTs composite

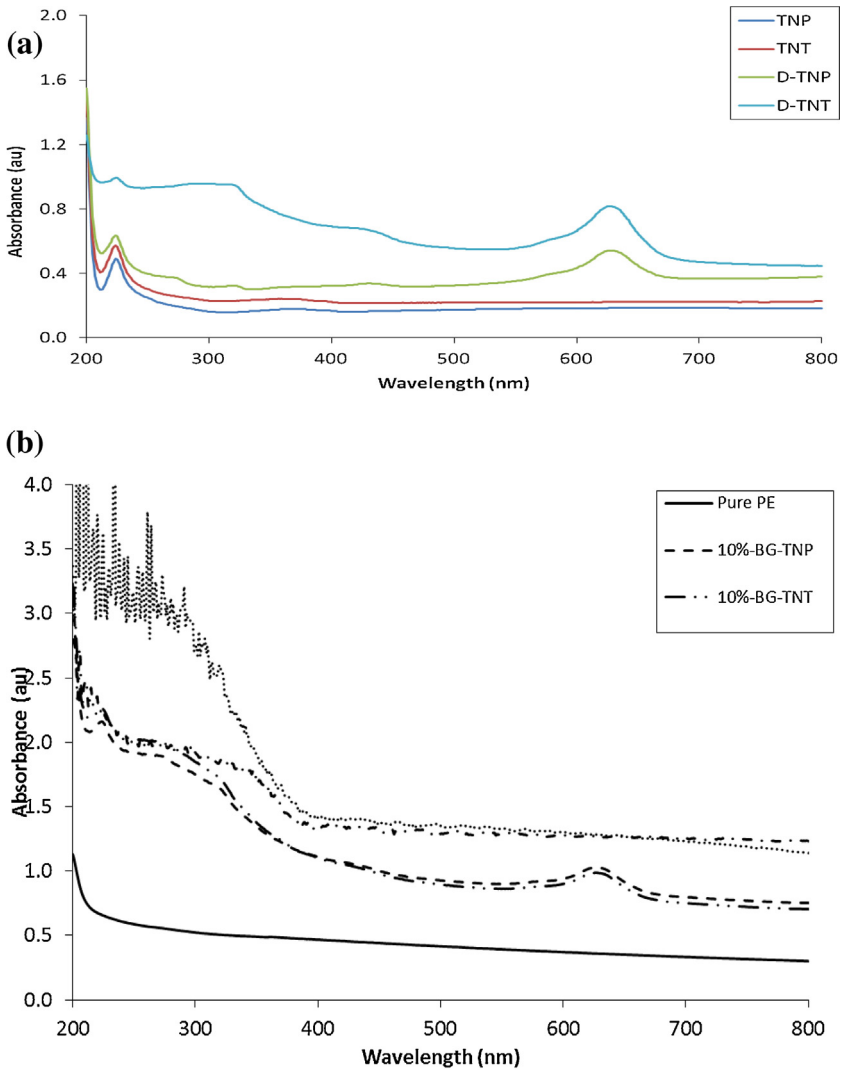

Fig. 4. (a) UV–visible spectrums of nanostructures (b) UV–visible spectrum of pure and composite films before and after irradiation exposure.

films after UV irradiation are shown in Fig. 3d and e respectively. Nanotubes composites showed larger cavities and more damage as compared to nanoparticles composites.

SEM images of LDPE composites after visible light exposure are shown in Fig. 3(f–i). The surfaces of those films which contain BG sensitized NPs or NTs are more damaged than LDPE films containing pure NPs or NTs. These composite films showed some cavities from degradation with large interconnected holes. LDPE and exposed TiO_2 interaction starts the photocatalysis process and leads to the formation of holes around TiO_2 nanotubes. Formation of volatile degradation products might have produced such cavities in films (Li et al., 2007). These results proved that degradation efficiency of BG-NTs is much better than pure TNPs. This result is according to weight loss shown in Fig. 5(a and b). The final degraded films are shown in Fig. 3l.

3.6. Spectroscopic analysis

3.6.1. UV–visible spectroscopy

Spectra of the dye adsorbed on pure and dye sensitized nanostructures was taken by rubbing the powder sample on a piece of transparent paper and placing it into the optical path of built-in cell holder of the spectrophotometer (same piece of blank paper was used as a reference). Fig. 4(a) shows the UV–vis spectra of pure and dye sensitized nanoparticles and nanotubes. Pure TNPs or TNTs absorbs UV light and generate mobile electron e^- in the conduction band and holes h^+ in the valence band where adsorbed oxygen species react with these electrons and produce reactive oxygen species like O^{2-}, O and O^-. On the other side, BG sensitized nanostructures showed absorbance in visible range (Zhao et al., 2008). Fig. 4(b) shows the absorbance spectras of pure LDPE and composite films before and after irradiation. Pure film showed less absorbance in visible as well as in UV range but TiO_2 embedded films showed absorbance in UV range and dye sensitized TiO_2 composite films showed absorbance in visible range as well. Nanotubes exhibit more absorbance than nanoparticles. But after visible irradiation exposure, absorbance of TiO_2 composites enhanced because films became whitish perhaps due to light scattering, with continuous light exposure causing LDPE chains breaking and deterioration.

3.6.2. FT-IR spectrum

FT-IR spectra were used to examine the photo-catalytic degradation of films. Measurement range was 4000–450 cm^{-1}, It was observed that pure LDPE films showed characteristics peaks in the region of 1460 cm^{-1} (revealing a bending deformation) 2919 cm^{-1}, 2857 cm^{-1} (assignable to CH_2 as an asymmetric stretching) and 719 cm^{-1} (indicates a rocking deformation) which are same in all films showing that irradiation exposure does not change the chemical properties of LDPE films (Mouallif et al., 2011) as shown in Fig. 6. The spectra of composite LDPE films showed new peaks after

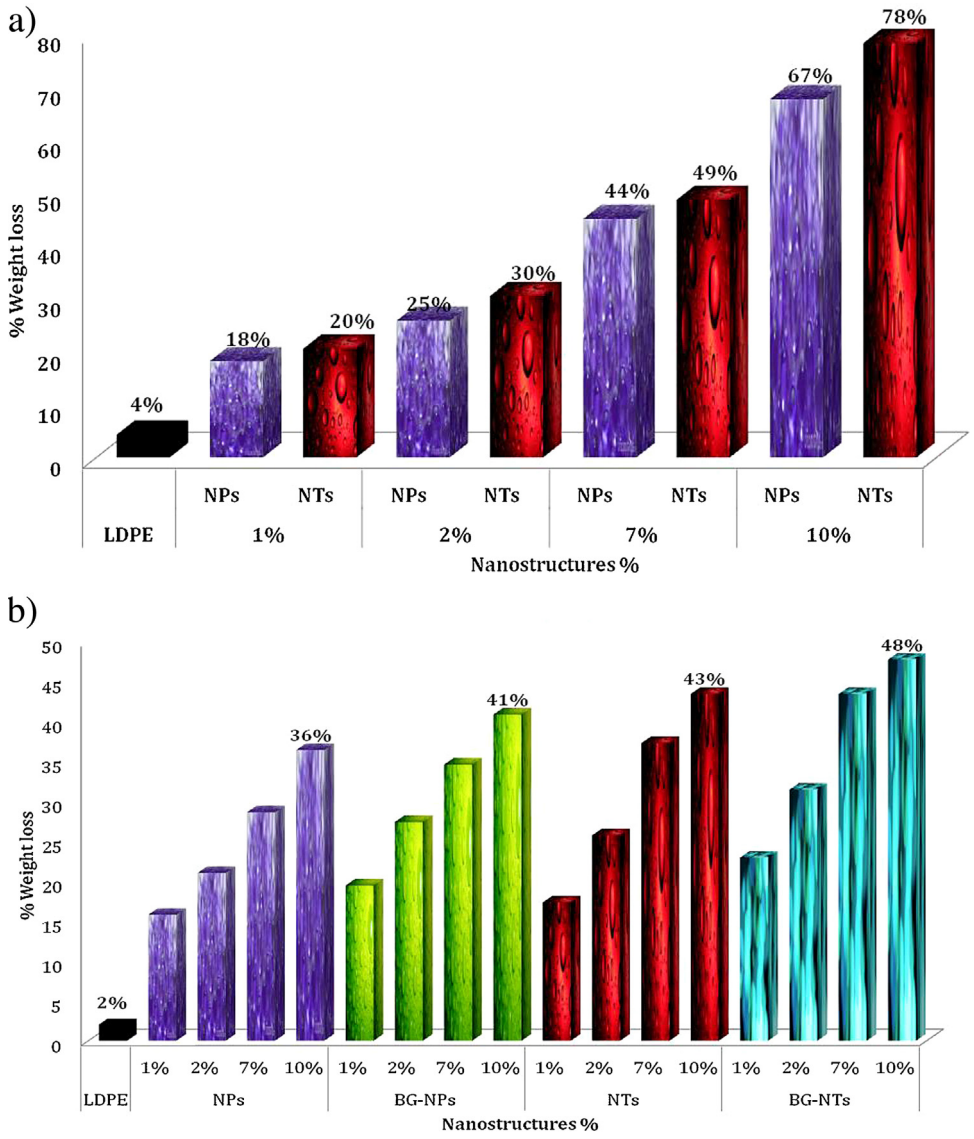

Fig. 5. (a) Comparison of weight loss of pure and LDPE composites under UV light where nanotubes showed faster degradation as compare to Titania nanoparticles (b) Comparison of weight loss of pure and LDPE composites under visible light.

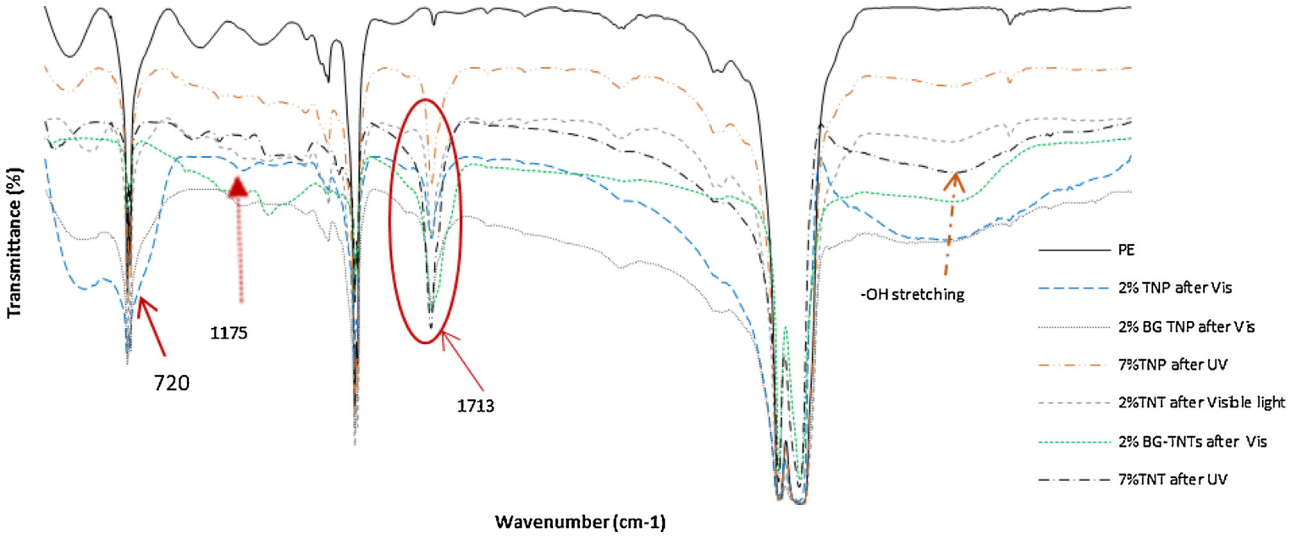

Fig. 6. Comparison between FTIR spectra of different LDPE composite films after irradiation.

Table 6
Carbonyl index of pure LDPE and composite films after irradiation.

Films composition	Carbonyl index [C=O: CH_2]
LDPE	0.33
2%TNPs after vis	1.2
2% BG TNPs after vis	1.25
2% TNPs after UV	1.48
2%TNTs after vis	1.39
2% BGTNTs after vis	1.52
2%TNTs after UV	2.00

irradiation around 1713 cm^{-1}, 1178 cm^{-1} and 1631 cm^{-1} which could be due to the carbonyl group (C=O) and C—O, C=C a stretching vibrations, respectively (Asghar et al., 2011; Li et al., 2007). —OH stretching region of hydroxylic group 3100–3600 showed increment in the films as highlighted in Fig. 6. It has been reported earlier that an increase in the —OH stretching region of hydroxylic group 3050–3570 is due to formation of hydroperoxide and alcohol during photo-oxidation (Guadagno et al., 2001). These alterations in spectra proved the structural alterations in LDPE films while degrading.

3.6.3. *Carbonyl index method*

To quantify the degree of photo-oxidation in polyethylene films, carbonyl index which is the ratio of absorbance of carbonyl group around 1710 cm^{-1} to an internal thickness band as reference peak at 1380 cm^{-1} is commonly used (Angulo-Sanchez et al., 1994; Salem, 2001).

$$\text{Carbonyl index (C.I)} = \frac{\text{A1710}}{\text{A1380}}$$

Table 6 shows the carbonyl index of the LDPE and composite films, showing an increase after irradiation. The carbonyl index for LDPE composites which contain TNTs is higher than TNPs composites. Also TNTs enhance the carbonyl index from 0.33 to maximum of 2.0 under UV light.

3.7. *Proposed LDPE photo-degradation mechanism*

Photocatalytic degradation of LDPE is only stimulated by UV light due to presence of C—C and C—H bonds in polyethylene. The wavelength of UV light is in range of 200–390 nm which form macromolecular radicals due to the as holes and electrons centers after reacting with LDPE. Water and oxygen reacts with these electrons or holes to create active oxygen species leading to the chain cleavage and oxidation reactions. These oxygenated species such as OH and $O_2^{\bullet -}$ are initiators of LDPE degradation by attacking the polymeric chain (Fa et al., 2010; Zan et al., 2006; da Silva et al., 2014; IKADA, 1993; Mucha et al., 2014; u Zhao et al., 2007).

Basically, degradation of LDPE gains momentum by the presence of alcoholic and carbonyl groups (Zan et al., 2006). It is proposed that in LDPE-(BG-TNPs or TNTs) composites, on titania nanostrucures, BG dye generates holes in ground state which takes part in degradation of LDPE matrix also with —OH and O_2.

$$h^+ + (CH_2CH_2)- \rightarrow -(CH_2CH_2)-^+$$

$$-(CH_2CH_2)-^+ + O^{2-} \rightarrow -(C^{\bullet}HCH_2)- + HO_2^{\bullet}$$

$$HO_2^{\bullet} + HO_2^{\bullet} \rightarrow H_2O_2 + O_2$$

$$H_2O_2 \xrightarrow[hv]{} 2^{\bullet}OH$$

The composites with BG-TiO_2 can produce more —OH to photodegrade polymer matrix. Monitoring of carbonyl groups helps to determine the degradation rate of PE. The damaging effects caused due to photo-oxidative degradation can be noted visually like yellowing, PE loss their mechanical properties and molecular weight get change (Singh and Sharma, 2008).

TiO_2 photosensitization starts when photons excites dye molecules which are adsorbed on TiO_2 and forms cationic radicals by injecting electrons from valence band to conduction band of TiO_2. Reactive species like H_2O_2, O_2 and OH thus produced allow the injected electrons react with O^{2-} absorbed on TiO_2 surface which ultimately help to degrade target pollutants (Li et al., 2012).

4. Conclusions

This study demonstrated the photocatalytic degradation process of BG sensitized TNTs composite PE films under visible light exposure. Dye sensitization of nanostructures has increased the degradation rate of LDPE films under visible light and those films can degrade under sunlight with good rate. Volatile organic product generation during photo-degradation produces defects in films which are confirmed by FTIR, SEM and tensile strength measurements. This new LDPE-TNTs composite is an environmental friendly polymer material which could be degraded when exposed to the outdoor environment.

Conflict of interest

We have read and understood journal policy on declaration of interests and declare that we have no competing interests. The authors acknowledge National University of Science and technology for providing the facility and financial support.

References

Akarsu, M., Asilturk, M., Sayilkan, F., Kiraz, N., Arpac, E., Sayilkan, H., 2006. A novel approach to the hydrothermal synthesis of anatase titania nanoparticles and the photocatalytic degradation of rhodamine B. Turk. J. Chem. 30 (3), 333–343.
Angulo-Sanchez, J.L., Ortega-Ortiz, H., Sanchez-Valdes, S., 1994. Photodegradation of polyethylene films formulated with a titanium-based photosensitizer and titanium dioxide pigment. J. Appl. Polym. Sci. 53 (7), 847–856.
Asapu, R., Palla, V.M., Wang, B., Guo, Z., Sadu, R., Chen, D.H., 2011. Phosphorus-doped titania nanotubes with enhanced photocatalytic activity. J. Appl. Polym. Sci. Chem. 225 (1), 81–87.
Asghar, W., Qazi, I.A., Ilyas, H., Khan, A.A., Awan, M.A., Aslam, M.R., 2011. Comparative solid phase photocatalytic degradation of polythene films with doped and undoped TiO_2 nanoparticles. J. Nano Mat. 2011, 12.
Briassoulis, D., 2006. Mechanical behavior of biodegradable agricultural films under real field conditions. Polym. Degrad. Stab. 91 (6), 1256–1272.
Briassoulis, D., Aristopoulou, A., Bonora, M., Verlodt, I., 2004. Degradation characterisation of agricultural low-density polyethylene films. Biosyst. Eng. 88 (2), 131–143.
Chakrabarti, S., Chaudhuri, B., Bhattacharjee, S., Das, P., Dutta, B.K., 2008. Degradation mechanism and kinetic model for photocatalytic oxidation of PVC–ZnO composite film in presence of a sensitizing dye and UV radiation. J. Hazard. Mater. 154 (1), 230–236.
Chappard, D., Degasne, I., Hure, G., Legrand, E., Audran, M., Basle, M.F., 2003. Image analysis measurements of roughness by texture and fractal analysis correlate with contact profilometry. Biomaterials 24 (8), 1399–1407.
Chatterjee, D., Mahata, A., 2001. Demineralization of organic pollutants on the dye modified TiO_2 semiconductor particulate system using visible light. Appl. Catal. B Env. 33 (2), 119–125.
Chatterjee, D., Dasgupta, S., Rao, N.N., 2006. Visible light assisted photodegradation of halocarbons on the dye modified TiO_2 surface using visible light. Sol. Energy Mater. Sol. Cells 90 (7), 1013–1020.
Chowdhury, P., Moreira, J., Gomaa, H., Ray, A.K., 2012. Visible-solar-light-driven photocatalytic degradation of phenol with dye-sensitized TiO_2: parametric and kinetic study. Ind. Eng. Chem. Res. 51 (12), 4523–4532.
da Silva, K.I.M., Fernandes, J.A., Kohlrausch, E.C., Dupont, J., Santos, M.J.L., Gil, M.P., 2014. Structural stability of photodegradable poly (L-lactic acid)/PE/TiO_2 nanocomposites through TiO_2 nanospheres and TiO_2 nanotubes incorporation. Polymer Bull. 71 (5), 1205–1217.
da Silva, K.I., Santos, M.J., Gil, M.P., 2015. Dependence of the photodegradation rate on the crystalline portion of PE films obtained through in situ polymerization in the presence of TiO_2 nanospheres, nanoribbons and microspheres. Polym. Degrad. Stab. 112, 78–85.
Fa, W., Yang, C., Gong, C., Peng, T., Zan, L., 2010. Enhanced photodegradation efficiency of polyethylene-TiO_2 nanocomposite film with oxidized polyethylene wax. J. Appl. Polym. Sci. 118 (1), 378–384.

Fostier, A.H., Pereira, M.D.S.S., Rath, S., Guimarães, J.R., 2008. Arsenic removal from water employing heterogeneous photocatalysis with TiO_2 immobilized in PET bottles. Chemosphere 72 (2), 319–324.
Gelover, S., Mondragón, P., Jiménez, A., 2004. Titanium dioxide sol–gel deposited over glass and its application as a photocatalyst for water decontamination. J. Photochem. Photobiol. A Chem. 165 (1), 241–246.
Guadagno, L., Naddeo, C., Vittoria, V., Camino, G., Cagnani, C., 2001. Chemical and morphological modifications of irradiated linear low density polyethylene (LLDPE). Polym. Degrad. Stab. 72 (1), 175–186.
Ikada, E., 1993. Role of The molecular structure in the photodecomposition of polymers. J. Photopolym. Sci. Technol. 6 (1), 115–122.
Kato, S., Hirano, Y., Iwata, M., Sano, T., Takeuchi, K., Matsuzawa, S., 2005. Photocatalytic degradation of gaseous sulfur compounds by silver-deposited titanium dioxide. Appl. Catal. B Env. 57 (2), 109–115.
Khan, S., Qazi, I.A., Hashmi, I., Ali Awan, M., Zaidi, N.U.S.S., 2013. Synthesis of silver-doped titanium TiO_2 powder-coated surfaces and its ability to inactivate pseudomonas aeruginosa and bacillus subtilis. J. Nano Mat. 8.
Kim, D.K., Zhang, Y., Voit, W., Rao, K.V., Muhammed, M., 2001. Synthesis and characterization of surfactant-coated superparamagnetic monodispersed iron oxide nanoparticles, J. Magn. Magn. Mater. 225 (1), 30–36.
Kim, S.H., Kwak, S.Y., Suzuki, T., 2006. Photocatalytic degradation of flexible PVC/TiO_2 nanohybrid as an eco-friendly alternative to the current waste landfill and dioxin-emitting incineration of post-use PVC. Polymer 47 (9), 3005–3016.
Latif, W., Qazi, I.A., Hashmi, I., Arshad, M., Nasir, H., Habib, A., 2014. Novel method for preparation of pure and iron-doped titania nanotube coated wood surfaces to disinfect airborne bacterial species *Pseudomonas aeruginosa* and *Staphylococcus aureus*. Environ. Eng. Sci. 31 (12), 681–688.
Li, X., Wang, D.T., Chen, J.F., Tao, X., 2012. Enhanced photosensitized phase degradation of organic pollutants under visible radiation by (I2) n-encapsulated TiO_2 films. Ind. Eng. Chem. Res. 51 (3), 1110–1117.
Li, Z., Chen, Y., Shi, L., Zhu, Y., 2007. Solid-phase photocatalytic degradation of polyethylene plastic under UV and solar light irradiation. J. Mol. Catal. A Chem. 268 (1), 101–106.
Liang, W., Luo, Y., Song, S., Dong, X., Yu, X., 2013. High photocatalytic degradation activity of polyethylene containing polyacrylamide grafted TiO_2. Polym. Degrad. Stab. 98 (9), 1754–1761.
Macák, J.M., Tsuchiya, H., Ghicov, A., Schmuki, P., 2005. Dye-sensitized anodic TiO_2 nanotubes. Electrochem. Commun 7 (11), 1133–1137.
Mehmood, C.T., Qazi, I.A., Baig, M.A., Arshad, M., Qudos, A., 2015. Application of photodegraded polythene films for the treatment of drimarene brilliant red (DBR) dye. Int. Biodeterior. Biodegrad. 1–9, http://dx.doi.org/10.1016/j.ibiod.2014.12.014.
Mouallif, I., Latrach, A., Benali, A., Barbe, N., (2011). FTIR study of HDPE structural changes, moisture absorption and mechanical properties variation when exposed to sulphuric acid aging in various temperatures. 20ème Congrès Français de Mécanique, 28 aoÛt/2 sept Besançon, France (FR). 2011-25044.
Mucha, M., Bialas, S., Kaczmarek, H., 2014. Effect of nanosilver on the photodegradation of poly (lactic acid). J. Appl. Polym. Sci. 131 (8).
Njeru, J., 2006. The urban political ecology of plastic bag waste problem in Nairobi. Kenya. Geoforum. 37, 1046–1058.
Salem, M.A., 2001. Mechanical properties of UV-irradiated low-density polyethylene films formulated with carbon black and titanium dioxide. Egypt. J. Sol. 24 (2), 141–150.
Seymour, R.B., 1989. Polymer science before and after 1899: notable developments during the lifetime of Maurits Dekker. J. Macromol. Sci. Chem. 26 (8), 1023–1032.
Shah, A.A., Hasan, F., Hameed, A., Ahmed, S., 2008. Biological degradation of plastics: a comprehensive review. Biotechnol. Adv. 26 (3), 246–265.
Sheavly, S.B., Register, K.M., 2007. Marine debris & plastics: environmental concerns, sources, impacts and solutions. J. Polym. Environ. 15 (4), 301–305.
Singh, B., Sharma, N., 2008. Mechanistic implications of plastic degradation. Polym. Degrad. Stab. 93 (3), 561–584.
Thomas, R.T., Nair, V., Sandhyarani, N., 2013. TiO_2 nanoparticle assisted solid phase photocatalytic degradation of polythene film A mechanistic investigation. Colloid Surf. A 422, 1–9.
Tomás, S.A., Zelaya, O., Palomino, R., Lozada, R., García, O., Yáñez, J.M., Ferreira da Silva, A., 2008. Optical characterization of sol gel TiO_2 monoliths doped with brilliant green. Eur. Phys. J. Spec. Top. 153 (1), 255–258.
u Zhao, X., Li, Z., Chen, Y., Shi, L., Zhu, Y., 2007. Solid-phase photocatalytic degradation of polyethylene plastic under UV and solar light irradiation. J. Mol. Catal. A 268 (1), 101–106.
Vinu, R., Polisetti, S., Madras, G., 2010. Dye sensitized visible light degradation of phenolic compounds. Chem. Eng. J. 165 (3), 784–797.
Wang, J., Lin, Z., 2009. Dye-sensitized TiO_2 nanotube solar cells with markedly enhanced performance via rational surface engineering. Chem. Mater. 22 (2), 579–584.
Wong, C.L., Tan, Y.N., Mohamed, A.R., 2011. A review on the formation of titania nanotube photocatalysts by hydrothermal treatment. J. Environ. Manage. 92 (7), 1669–1680.
Yuan, F., Li, P., Qian, H., 2013. Photocatalytic degradation of polyethylene glycol by nano-titanium dioxide modified with ferric acetylacetonate. Synth. React. Inorg. Met. Org. Chem. 43 (3), 321–324.
Zan, L., Fa, W., Wang, S., 2006. Novel photodegradable low-density polyethylene-TiO_2 nanocomposite film. Environ. Sci. Technol. 5, 1681–1685.
Zhao, X., Li, Z., Chen, Y., Shi, L., Zhu, Y., 2008. Enhancement of photocatalytic degradation of polyethylene plastic with CuPc modified TiO_2 photocatalyst under solar light irradiation. Appl. Surf. Sci. 254 (6), 1825–1829.
Zhiyong, Y., Mielczarski, E., Mielczarski, J., Laub, D., Buffat, P., Klehm, U., Kiwi, J., 2007. Preparation, stabilization and characterization of TiO_2 on thin polyethylene films (LDPE) Photocatalytic applications. Water Res. 41 (4), 862–874.